B. ONLINE Appendix

Estimating macro-fiscal effects of climate shocks from billions of geospatial weather observations

by Berkay Akyapı, Matthieu Bellon, and Emanuele Massetti[25]

B.1. Source Data

We use weather from the ERA5 dataset from 1979 to 2021.[26] The original ERA5 dataset has hourly data but we use data aggregated at daily level by Google Earth Engine (GEE).[27] This includes daily mean temperature in each day d and grid cell j, calculated using ERA5's 24 measures per day ($T_{j,d}$), the minimum of those 24 measures within a day ($TN_{j,d}$), and the maximum of those 24 measures within a day ($TX_{j,d}$). Total daily precipitation ($P_{j,d}$) is calculated by summing all the hourly precipitation measures within a day. From these daily grid-cell data points we construct all our variables.

Number of observations in the original databases. The resolution of ERA5 data is 0.25 degrees. A global map has 180 degrees along the North-South dimension and 360 degrees along the West-East dimension: the total number of cells is therefore equal to $(180/0.25) \times (360/0.25) = 1,036,800$. The percentage of Earth's surface covered land, after excluding Antarctica and Greenland, is approximately equal to 27%. This means that we use approximately 1,036,800 × 0.27 = 279,936 cells on land. For each grid and each day of the 41 years from 1979 to 2019 we have four weather data points (T, TN, TX, and P). This means that we start with approximately 279,936 × 365 × 41 × 4 = 16,756,968,960 (≈ 17 billion) temperature and precipitation data points.

The Palmer Drought Severity Index (PDSI) is from Abatzoglou et al. (2018) and is accessed using GEE.[28] PDSI data comes at monthly intervals with spatial resolution equal to 0.0416 degrees. This corresponds to (180 / .0416) × (360 / 0.0416) × 0.27 = 10,110,022 cells on land excluding Antarctica and Greenland. Summing over all months from January 1979 to December 2019 we have a total of 10,110,022 × 12 × 41 = 4,974,130,917 (≈ 5 billion) observations on PDSI from the Terra Climate data.

To sum up, we start with 21,715,195,392 (≈ 22 billion) data points on temperature, precipitation, and the PDSI.

Merging datasets and zonal statistics. We merge the ERA5 and PDSI datasets into one single geospatial dataset that uses the higher resolution of PDSI data of approximately 5 km × 5 km at the

[25]Akyapı: berkayakyapi@ufl.edu; Bellon: m.bellon@esm.europa.eu; Massetti: emassetti@imf.org

[26]`https://cds.climate.copernicus.eu/cdsapp#!/dataset/reanalysis-era5-single-levels?tab=overview`

[27]`https://developers.google.com/earth-engine/datasets/catalog/ECMWF_ERA5_DAILY#description`

[28]`https://developers.google.com/earth-engine/datasets/catalog/IDAHO_EPSCOR_TERRACLIMATE#bands`

equator. This dataset is projected on a global map of countries to calculate zonal statistics at country level.[29] The whole process is managed using Google Earth Engine and delivers a total of 9,621,976 ($\approx$ 10 million) country-matched grid cells for each one of our five core climate variables ($T_{j,d}$, $TN_{j,d}$, $TX_{j,d}$, $P_{j,d}$, and $PDSI_{j,d}$). Each grid cell has daily data for 41 years. This means we develop our full set of climate variables using 580,705,495,552 ($\approx$ 600 billion) data points.

Weighted variables. The resolution for the population data is $\approx$ 1 km $\times$ 1 km at the equator,[30,31] and hence for the weighted data we use 1 km $\times$ 1 km grid cells during zonal statistics. By mixing population and weather data we obtain 25 additional points for each grid cell of the raw weather data. This adds 25 $\times$ 580,705,495,552 = 14,517,637,388,800 ($\approx$ 15 trillion) data points to our dataset for zonal statistics.

B.2. Definition of weather variables

This Section describes all the weather variables we construct from raw precipitation and temperature data. We start by an overview of weather variables, then give a brief presentation of mathematical notations and concepts, and finally provide the full list of the variables we construct and their mathematical definitions in table A.1.

Temperature variables. For each day in a year and country, we calculate country-wide averages of daily average, minimum, and maximum temperature (respectively T_d, TN_d, and TX_d) from daily grid level data. We aggregate average daily temperatures to get annual average temperature (T), the variance of daily temperature ($TVar$). We calculate the average diurnal temperature range (DTR) from minimum and maximum daily temperatures. Using the 10^{th} and 90^{th} percentiles of the 1979-2019 distribution of TN_d and TX_d in a 5-day window centered on each day of the year, we calculate the number of cold nights ($CN10$), cold days ($CD10$), warm nights ($WN90$) and warm days ($WD90$), to characterize cold and heat extremes using relative thresholds.

To account for impacts from extended exposure to temperature extremes, we build variables to capture heatwaves and coldwaves based on the climate literature. We follow Kim et al. (2020) and we define cold (warm) spell duration (CSD, WSD) as the number of days in which TN_d (TX_d) is below (above) the 10^{th} (90^{th}) percentile of the 1979-2019 distribution in a 5-day window centered on each day, for at least six consecutive days. We follow Perkins and Alexander (2013) to define eight additional indicators of day (night) heat waves based on exceeding the 90^{th} percentile of the 1979-2019 distribution of TX_d (TN_d) in a 15-day window centered on each day, for at least three consecutive days. We count the number of days with day (night) heat wave, the length of the longest day (night) heatwave, the number of day (night) heatwaves during a year, and the average maximum (minimum) temperature during day (night)

[29] Zonal statistics are operations that calculate statistics of cell values of a dataset (raster) within boundaries defined by another dataset.

[30] `https://doi.org/10.7927/H4F47M65`

[31] `https://developers.google.com/earth-engine/datasets/catalog/CIESIN_GPWv411_GPW_UNWPP-Adjusted_Population_Count`

heatwaves. Similarly, we use the 10^{th} percentile of the distribution of TX_d and TN_d to measure the characteristics of day and night cold waves.

We construct country averages of grid-level annual minimum of minimum daily temperature (TNn) and of grid-level maximum of maximum daily temperature (TXx), both used in the climate literature.

We also define another set of extreme temperature variables using absolute temperature thresholds based on the climate literature (e.g., IPCC, 2021a). With absolute temperature thresholds, using the highest possible level of spatial resolution is essential to avoid missing the potentially harmful events that can get averaged out over large areas. For example, if two grid cells have maximum daily temperature equal to, respectively, 33 °C and 36 °C, their average is equal to 34.5 °C, lower than the frequently used 35 °C threshold. By first averaging and then checking if the threshold is crossed, we would record zero extreme events, while temperature in 50% of the grid cells exceeds the threshold. The same does not apply to extremes measured using relative thresholds.

Therefore, when we use absolute thresholds, we sum the number of times a threshold is crossed in each grid cell and in each day, across all days and grid cells in a country, and then divide that number by the total number of grid-day observations ($J \times 365$). We do so to find the share of grid-days with frost (minimum daily temperature below 0°C – $TN0$), with maximum temperature above 35 °C ($TX35$) and above 40°C ($TX40$).

Finally, to capture potential non-linear effects of temperature on macroeconomic variables, we divide the distribution of temperature into 3 °C-wide intervals and we measure the share of grid-day observations in each interval (e.g., Schlenker and Roberts, 2009). For example, Figure B.1 illustrates the calculation of the share of grid-days that experiences temperature levels between x_1 and x_2 degrees Celsius. By using 3 °C wide intervals we aim to balance flexibility in modeling the temperature response function and avoiding multicollinearity problems that would arise from using narrower temperature intervals (Mérel and Gammans, 2021). One of the intervals is omitted in our estimation process to avoid perfect collinearity among all interval indicators. As very low and very high average daily temperatures are rare, all the days with average temperature below -9 °C and at or above 30 °C are grouped in two terminal intervals.

Precipitation (rain or snow) variables. We start by calculating the average of total daily precipitation in each country across all grid cells (P_d). We use this variable to construct annual average precipitation (P) and the annual variance of daily precipitation ($PVar$) for every country. Following the climate literature, we focus on days that have more than 1 mm of precipitation, which are called "wet days". We calculate the number of wet days (W), average daily precipitation in wet days (PWA), and wet days precipitation variance ($PWVar$). We calculate total precipitation in very wet ($PW95T$) and extremely wet days ($PW99T$) using the 95^{th} and 99^{th} percentiles of the distribution of wet days over all days and years from 1979 to 2019.

Figure B.1: Computing the share of grid-days with weather conditions in a specific interval

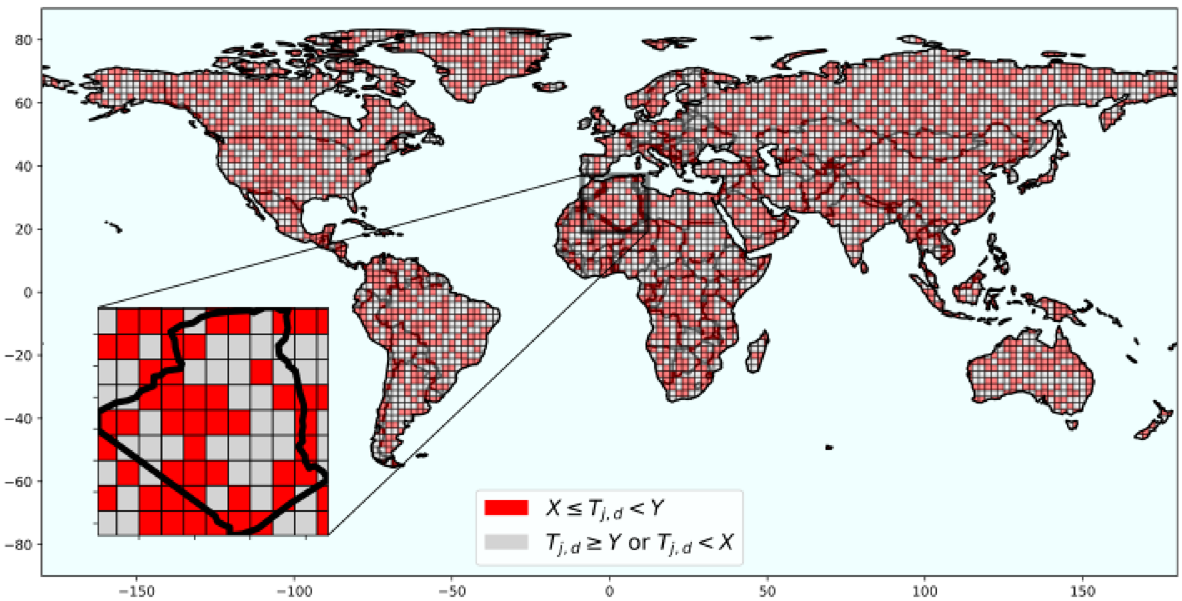

Notes: This figure illustrates the calculation methodology for "Share of Grid-Days with Mean Temperature in the interval $[x_1, x_2)$*" (Mean* $T\ ^\circ C$ *in* $[x_1, x_2)$ *—* $TS_{[x_1,x_2)}$*) for a given day d in any country j. We also zoom on Algeria. The grid cells colored in red represent the locations where* $x_1 \leqslant T_{j,d} < x_2$ *and grid cells colored in gray represent the locations where* $T_{j,d}$ *(average daily temperature in country j on day d) is outside of this range. For our study, we later obtain country-year measures by averaging daily percentages over the 365 days of a year. Note that the grid cells are pictured as much bigger than they are in the original dataset for visualization purposes. For example, there are 50 grid cells belonging to Algeria in this figure. However, there are more than 105 thousand grid cells in Algeria in the dataset.*

We build several variables to capture extended wet and dry periods. We count the largest number of consecutive dry days (days with precipitation less than 1 mm — CDD), the largest number of consecutive wet days (CWD) and total precipitation during the longest wet days period ($PCWD$). To focus on extreme conditions, we count the number of consecutive very ($PC95WD$) and extremely ($C99WD$) wet days in the longest periods with daily precipitation above the 95^{th} and 99^{th} percentiles of the distribution, respectively. Similarly, we calculate total precipitation in consecutive very ($PC95W$) and extremely wet days ($PC99WD$).

To capture intense precipitation that may cause floods, which are among the most destructive climate disasters, we use the maximum amount in a year of rainfall in 1-day ($PX1$) or 5-day ($PX5$) intervals. To capture extreme precipitation at the local level, we use total monthly precipitation in each grid cell and we calculate the country average of maximum ($PX(1Month)$) and minimum ($PN(1Month)$) monthly precipitation.

As for temperature, precipitation extremes can also be characterized using absolute thresholds but this requires calculations at the grid level. We calculate the length of the longest dry spell ($LLDS$) in a country as the uninterrupted series of days in which a minimum percent of the country area has daily total precipitation less than 1 mm (dry day). We use four thresholds to identify dry spells and consider spells affecting 50%, 65%, 80% and 95% of a country area. Similarly to what we do with temperature intervals, we calculate the share of total grid-days with total precipitation in four intervals: less than 1 mm, from 1 mm to 10 mm, from 10 mm to 20 mm, and above 20 mm. The maximum extent of heavy ($MaxP_{>10}$) and very heavy ($MaxP_{>20}$) precipitation is equal to the maximum daily share of the country with precipitation respectively greater than 10 mm and 20 mm. To capture deviations from conditions with balanced level of precipitation across time and space, we develop an indicator that measures the absolute deviation from having 50% of the grid-days observations of precipitation between 1 and 10 mm ($BP_{1\_10}(0.5)$).

Wetness and drought variables. Finally, we use the Palmer Drought Severity Index (PDSI) (Palmer, 1965) to introduce a measure of dry and wet periods that combines temperature and precipitation data to estimate cumulative deviations in soil moisture from normal conditions (Dai et al., 2004; Abatzoglou et al., 2018; Lai et al., 2020).[32] The PDSI ranges from -10 to +10, but values below -4 and above +4 are rare. We build variables measuring the share of total grid-months subject to extreme droughts (PDSI < -4), extreme and severe droughts (PDSI < -3), periods with extreme moisture (PDSI > 4), and periods with very high and extreme moisture (PDSI > 3). For each of these four categories and in every country, we also build variables reflecting the maximum extent of these events, that is the share of affected grid-cells in the month where the share is at its maximum.

Mathematical notations and concepts. We use d to denote calendar days, months with m, and $j = 1, \ldots, J$ to denote grid cells in every country. For ease of notation, we do not index variables by country and year. In each year there are 12 months and for ease of notation we assume each year has the same number of days.

We use Iverson brackets in the definition of many variables. Iverson brackets map any statement inside brackets into a function that takes the value of the variables for which the statement is true, and take the value zero otherwise.[33] It is denoted by putting the statement inside square brackets:

$$[X] = \begin{cases} 1 & \text{if } X \text{ is true;} \\ 0 & \text{otherwise.} \end{cases}$$

Thus, to count days in which a certain condition X is met we write: $\sum_d [X]$.

Some variables capture different percentiles of the long-term distribution of daily mean temperature and daily precipitation. We use the whole time horizon of our dataset for these distributions, from 1979 to

[32] Data downloaded from Google Earth Engine. See `http://www.climatologylab.org/terraclimate.html` and `https://developers.google.com/earth-engine/datasets/catalog/IDAHO_EPSCOR_TERRACLIMATE` for a detailed description of the datasets.

[33] Donald Knuth, "Two Notes on Notation" American Mathematical Monthly, Volume 99, Number 5, May 1992, pp. 403–422.

2019. This is represents a 41-year time window that is well-suited to capture extreme realizations of temperature and precipitation.

For daily precipitation, we use all days of the calendar year as there are no obvious seasonal patterns that apply to all countries. For temperature, there is a more marked seasonal cycle in most countries and deviations from normal conditions are more clearly dependent on the time of the year temperature is observed. For this reason, the distribution of temperature is restricted to moving windows centered on the day of interest. We use 5-day and 15-day windows following the literature Kim et al. (2020); Perkins and Alexander (2013). For example, consider August 16, 2000. To check whether precipitation is extreme, we compare daily precipitation with the distribution of precipitation over all days from 1979 to 2019. To check if temperature is extreme, we restrict the distribution of daily mean temperature to August 14, 15, 16, 17, and 18 (with a 5-day window) from 1979 to 2019.

B.3. Summary Statistics

Between and within variance. Our empirical and identification approach relies on inter-annual variation within country. Therefore, we use a standard approach to decompose the variance of variables into *between* and *within* components.

For any variable x, the variance across N countries and over T years can be decomposed by introducing country averages $\bar{x}_i$. The variance is equal to $\sum_{i,t} \frac{(x_{i,t}-\bar{x})^2}{NT} = \sum_{i,t} \frac{(x_{i,t}-\bar{x}_i)^2}{NT} + 2\sum_{i,t} \frac{(x_{i,t}-\bar{x}_i)}{T}\frac{(\bar{x}_i-\bar{x})}{N} + \sum_{i,t} \frac{(\bar{x}_i-\bar{x})^2}{NT}$. It simplifies to $\sum_{i,t} \frac{(x_{i,t}-\bar{x})^2}{NT} = \sum_{i,t} \frac{(x_{i,t}-\bar{x}_i)^2}{NT} + \sum_{i} \frac{(\bar{x}_i-\bar{x})^2}{N}$ where the terms are respectively the within and between variance. We take the square roots of each component to obtain *between*- and *within*-country standard deviations.

The *between* standard deviation measures variation of average country weather around the global mean. The *within* standard deviation measures the average deviation from country averages.

Trends in weather variables. Table B.1 reports tests of trends in the levels of the weather variables. For each variable and each country we estimate a linear regression of the form $w_t = \alpha + \beta t + u_t$, where w_t is the value taken by the weather variable in year t, u_t is a random component and β is the country-specific trend coefficient.

Column A reports the average β across all countries. Our results are not truly indicative of global trends, because we use country-level observations instead of area-weighted averages. For an accurate assessment of climate trends, it is important to rely on conclusions from climate science (IPCC, 2021b). However, the positive trend for average annual temperature is equal to 0.03 °C per year, a value remarkably in line with the average decadal increase of temperature equal to 0.3 °C found by the IPCC WG I.

Column B shows the percentage of countries for which the trend is significantly different from zero at the 5 percent confidence level. We use this percentage value to rank variables in decreasing order. Most of the variables built using temperature show a significant trend consistent with global warming in the majority of countries, and in some cases in virtually all countries. Variables built using precipitation do not generally show a trend that is significant for the majority of countries and in most cases trends are not significant for more than 2/3 of the countries.

Our model specification (see equation (2)) effectively removes trends in climate variables only if the trend is time invariant. To assess weather trends change over time, we conduct a test for a structural trend break with unknown break date in the time series of each climate variable, separately in each country. In column C we report the percentage of countries with both a significant trend and a significant break in the trend.[34] There is evidence of a trend with a structural break for more than 50 percent of the countries only for few variables. This suggests that our method, albeit imperfectly, helps to remove trends in weather variables.

Table B.1: Trends in weather variables

	(A) Average trend	(B) Significant trend (% of countries)	(C) Significant trend and break (% of countries)
Mean Temperature	0.0292	99%	50%
# of Warm Nights	1.4904	97%	71%
# of Warm Days	1.3516	96%	62%
# of Cold Days	-1.0564	95%	51%
# of Cold Nights	-1.2086	94%	64%
# of Day Cold Waves	-0.0858	90%	46%
# of Night Heat Waves	0.1175	89%	65%
Cold Wave Days	-0.5272	89%	53%
Heat Wave Nights	0.7510	89%	62%
# of Day Heat Waves	0.1094	88%	57%
Heat Wave Days	0.6824	88%	60%
Cold Wave Nights	-0.5965	87%	57%
# of Night Cold Waves	-0.0979	87%	56%
Longest Day Heat Wave	0.1574	81%	47%
Mean T °C in [27; 30)	0.0018	80%	52%
Longest Night Heat Wave	0.1737	78%	49%
Max T °C above 35	0.0008	76%	42%
Day T °C Maximum	0.0322	75%	42%
Warm Spell Duration	0.4343	74%	53%
Longest Night Cold Wave	-0.1439	73%	54%
Longest Day Cold Wave	-0.1313	72%	42%
Cold Spell Duration	-0.3679	72%	56%
Mean T °C in [24; 27)	-0.0008	70%	54%
Frost prevalence	-0.0009	69%	33%
Night Heat Wave T °C	0.0785	67%	54%
Mean T °C in [21; 24)	-0.0006	66%	43%
Mean T °C above 30	0.0006	66%	35%

Continued on next page

[34]More precisely, we test if the null hypothesis of no structural break can be rejected at the 95 percent confidence level using a supremum Wald test which is the least restrictive among those commonly used.

Table B.1 (Continued): trends in weather variables

Day Heat Wave T °C	0.0748	58%	54%
Max T °C above 40	0.0003	58%	36%
Mean T °C in [-6; -3)	-0.0002	58%	39%
Diurnal T °C Range	0.0051	53%	68%
Mean T °C in [15; 18)	-0.0001	53%	36%
Mean T °C in [18; 21)	-0.0001	52%	36%
Mean T °C in [-3; 0)	-0.0002	48%	34%
Night T °C Minimum	0.0266	48%	39%
Mean T °C in [-9; -6)	-0.0002	45%	35%
Mean T °C in [0; 3)	-0.0002	44%	30%
Mean T °C in [12; 15)	-0.0001	41%	41%
Balanced PPT Indicator	0.0003	38%	63%
Mean T °C in [9; 12)	-0.0001	37%	37%
Night Cold Wave T °C	0.0039	36%	42%
Drought Intensity	0.0039	35%	75%
Less than 1 mm PPT	0.0006	35%	65%
Mean T °C in [3; 6)	-0.0001	35%	32%
# of Wet Days	-0.2077	34%	59%
Mean T °C in [6; 9)	0.0000	34%	33%
Day Cold Wave T °C	0.0155	32%	46%
Harsh Drought Intensity	0.0037	31%	63%
Drought Prevalence	0.0026	29%	61%
Above 20 mm PPT	0.0001	28%	50%
Very Wet Day PPT	1.6213	28%	46%
Wetness Intensity	0.0008	27%	73%
Precipitation Variance	0.1271	27%	42%
10 to 20 mm PPT	-0.0001	26%	57%
Harsh Drought Prevalence	0.0019	26%	48%
High Wetness Intensity	0.0016	26%	59%
Wet Day PPT Variance	0.1818	26%	38%
Wet Conditions	0.0011	25%	59%
Mean Wet Day PPT	0.0049	24%	48%
PPT Maximum	0.0003	24%	44%
Mean Precipitation	0.0008	23%	58%
Cont'd Wet Days	-0.1937	21%	41%
Very Wet Conditions	0.0012	21%	43%
Longest Dry Spell (.80)	0.0541	20%	40%
Cont'd Dry Days	0.0774	19%	35%
Longest Dry Spell (.65)	0.1109	19%	41%
Extremely Wet Day PPT	0.7905	19%	37%
1-Day PPT Maximum	0.1054	18%	37%
Cont'd Wet Day PPT	-0.6595	18%	37%
5-Day PPT Maximum	0.1418	17%	34%
PPT Minimum	0.0000	17%	31%
Longest Dry Spell (.95)	0.0241	15%	39%
Extreme PPT Maximum	0.0008	15%	36%
Longest Dry Spell (.5)	0.1123	15%	40%
Cont'd Heavy PPT	0.1693	14%	32%
Cont'd Very Wet Day PPT	0.0034	12%	32%
Temperature Variance	0.0046	12%	38%
Heavy PPT Maximum	0.0000	8%	33%
Cont'd Extreme PPT	0.1885	7%	18%
Cont'd Extra Wet Day PPT	0.0046	7%	20%

Macroeconomic variables. Summary statistics for the macro-fiscal variables used in our analysis are shown in Table B.2. The Table displays separately the growth rate of GDP per capita in the larger sample used for the analysis of weather impacts on GDP growth, and the growth rate of GDP per capita in the smaller sample used for the analysis of fiscal impacts.

Table B.2: Summary statistics of macro-fiscal variables

Summary Statistics of First Differences	N	Mean	St. Dev.	St. Dev. Between	St. Dev. Within
$\Delta \ln(GDP/POP)$ in GDP Growth Sample (p.c.)	6,653	1.726%	4.63%	1.77%	4.33%
$\Delta \ln(GDP/POP)$ in Fiscal Sample (p.c.)	3,890	2.005%	3.85%	1.55%	3.56%
Δ Revenue-to-GDP (p.p.)	3,890	0.064%	2.90%	0.71%	2.86%
Δ Expenditure-to-GDP (p.p.)	3,890	0.045%	3.61%	0.92%	3.56%
Δ Balance-to-GDP (p.p.)	3,890	0.019%	4.12%	0.71%	4.09%
Δ Debt-to-GDP (p.p.)	3,890	0.177%	8.1%	1.96%	7.9%
Δ Revenue (p.c.)	3,890	3.873%	11.6%	2.50%	11.4%
Δ Expenditure (p.c.)	3,890	3.867%	10.8%	2.51%	10.6%
Δ Debt (p.c.)	3,890	4.221%	16.3%	4.91%	15.8%

Notes: GDP per capita is measured by the difference of log GDP capita. Government revenue, Government expenditure and Government Debt growth are measured by the difference of log variables. All fiscal variables are measured as percentage of GDP and first differences are measured in percentage points.

Table B.3: Summary statistics of climate variables

Summary Statistics of First Differences	Mean	St. Dev. Between	St. Dev. Within
Harsh Drought Prevalence (W) ($PDSI < -4$)	0.0050	0.0097	0.1741
Max T above 35 °C (W) ($TX35$)	0.0006	0.0011	0.0205
Mean T in [9; 12) °C (TS_{9_12})	0.0000	0.0007	0.0159
Longest Day Cold Wave ($LDCW$)	-0.1130	0.2584	5.903
Mean Wet Day PPT (PWA)	0.0025	0.0531	0.9897
PPT Minimum (PNM)	0.0000	0.0007	0.0161

Notes: Summary statistics of first differences of all weather variables used for either GDP analysis, including robustness tests, or for analysis of macro-fiscal outcomes. (W) indicates population-weighted variables. The sample of the baseline specification is used for all climate variables.

Correlation analysis. The analysis of raw correlations between GDP growth and the explanatory variables selected by the LASSO for our main specification is displayed in Table B.4. Correlations between GDP growth and first differences of weather variables are generally small. Correlation is negative for Max T °C above 35 and Harsh Drought Prevalence, and positive for Mean T °C in [9; 12). The same relationships are confirmed in our baseline regression analysis (see Table 1).

We also display the correlation of GDP growth with both average annual temperature and annual precipitation even if these two variables are not selected by the LASSO because they are the only two weather variables typically used in the literature. The correlation between GDP growth and both temperature and precipitation is very low and much lower than for our selected weather variables. This is preliminary evidence that the literature may miss a large fraction of climate induced variation in GDP growth. Interestingly, the largest correlations among climate variables are between Average Temperature and Harsh Drought Prevalence and between Mean Temperature and Max T °C above 35, but the LASSO always selects Harsh Drought Prevalence and Max T °C above 35 instead of Mean Temperature to explain GDP growth.

Table B.4: Correlation Matrix Between Baseline Variables

	GDP Growth	Lag(1) of GDP Growth	Lag(2) of GDP Growth	Harsh Drought Prevalence (W)	Max T °C above 35 (W)	Mean T °C in [9; 12)	Mean Temperature
Lag(1) of GDP Growth	0.366						
Lag(2) of GDP Growth	0.248	0.281					
Harsh Drought Prevalence (W) ($PDSI < -4$)	-0.058	0.025	0.012				
Max T above 35 °C (W) ($TX35$)	-0.040	0.016	0.021	0.180			
Mean T in [9; 12) °C (TS_{9_12})	0.040	-0.016	0.014	-0.032	-0.033		
Average T (T)	-0.015	0.020	-0.001	0.156	0.362	-0.053	
Mean Precipitation (P)	0.014	-0.006	-0.002	-0.196	-0.145	0.081	-0.087

Notes: These correlations are computed using first differences using the baseline regression sample. (W) indicates population-weighted variables.

Table B.5: Summary Statistics for Sub-Groups

	Mean	St. Dev. Between	St. Dev. Within	Mean	St. Dev. Between	St. Dev. Within
	Hot (N=3,315)			Cold (N=3,338)		
Δ GDP p.c.	1.38	1.85	4.44	2.07	1.59	4.22
Harsh Drought Prevalence (W) ($PDSI < -4$)	0.0032	0.0079	0.1668	0.0068	0.0108	0.1811
Max T above 35 °C (W) ($TX35$)	0.0008	0.0014	0.0257	0.0004	0.0007	0.0137
Mean T in [9; 12) °C (TS_{9_12})	-0.00006	0.0003	0.0041	0.0002	0.0009	0.0220
	Agricultural (N=3,119)			Non Agricultural (N=3,107)		
Δ GDP p.c.	1.71	1.77	4.55	1.75	1.46	3.89
Harsh Drought Prevalence (W) ($PDSI < -4$)	0.0043	0.0085	0.1833	0.0055	0.0091	0.1632
Max T above 35 °C (W) ($TX35$)	0.0009	0.0011	0.0257	0.0004	0.0008	0.0140
Mean T in [9; 12) °C (TS_{9_12})	0.00003	0.0005	0.0103	0.0001	0.0008	0.0193
	Agricultural Hot (N=1,785)			Agricultural Cold (N=1,334)		
Δ GDP p.c.	1.37	1.64	4.10	2.16	1.84	5.08
Harsh Drought Prevalence (W) ($PDSI < -4$)	0.0025	0.0062	0.1803	0.0067	0.0101	0.1872
Max T above 35 °C (W) ($TX35$)	0.0011	0.0012	0.0310	0.0006	0.0009	0.0160
Mean T in [9; 12) °C (TS_{9_12})	-0.0003	0.0001	0.0033	0.0001	0.0007	0.0153
	Rich (N=3,936)			Poor (N=2,717)		
Δ GDP p.c.	1.95	1.77	4.27	1.41	1.75	4.41
Harsh Drought Prevalence (W) ($PDSI < -4$)	0.0055	0.0102	0.1697	0.0042	0.0088	0.1803
Max T above 35 °C (W) ($TX35$)	0.0004	0.0008	0.0141	0.0010	0.0014	0.0273
Mean T in [9; 12) °C (TS_{9_12})	0.0001	0.0009	0.0194	0.0000	0.0002	0.0083
	EAP (N=1,013)			ECA (N=1,632)		
Δ GDP p.c.	2.42	2.23	3.89	2.31	1.48	4.49
Harsh Drought Prevalence (W) ($PDSI < -4$)	0.0017	0.0060	0.1683	0.0100	0.0112	0.1892
Max T above 35 °C (W) ($TX35$)	0.0006	0.0014	0.0240	0.0002	0.0004	0.0089
Mean T in [9; 12) °C (TS_{9_12})	-0.00004	0.0001	0.0054	0.0004	0.0011	0.0283
	MENA (N=620)			SSA (N=1,656)		
Δ GDP p.c.	0.97	1.86	5.16	1.07	1.52	4.66
Harsh Drought Prevalence (W) ($PDSI < -4$)	0.0003	0.0064	0.1961	0.0048	0.0096	0.1924
Max T above 35 °C (W) ($TX35$)	0.0011	0.0018	0.0246	0.0010	0.0012	0.0285
Mean T in [9; 12) °C (TS_{9_12})	-0.0003	0.0009	0.0196	-0.0001	0.0003	0.0052
	LAC (N=1,372)			Base (N=6,550)		
Δ GDP p.c.	1.36	1.47	3.87	1.73	1.77	4.33
Harsh Drought Prevalence (W) ($PDSI < -4$)	0.0056	0.0086	0.1388	0.0050	0.0097	0.1741
Max T above 35 °C (W) ($TX35$)	0.0005	0.0009	0.0122	0.0006	0.0011	0.0205
Mean T in [9; 12) °C (TS_{9_12})	-0.00002	0.0001	0.0056	0.0000	0.0007	0.0159
	High Democracy (N=3,895)			Low Democracy (N=2,753)		
Δ GDP p.c.	1.92	2.13	3.47	1.45	2.61	5.12
Harsh Drought Prevalence (W) ($PDSI < -4$)	0.0049	0.0180	0.1723	0.0049	0.0193	0.1758
Max T above 35 °C (W) ($TX35$)	0.0005	0.0031	0.0148	0.0008	0.0019	0.0265
Mean T in [9; 12) °C (TS_{9_12})	0.00006	0.0011	0.0186	0.0001	0.0013	0.0109

Continued on next page

Table B.5 (Continued): Summary Statistics for Sub-Groups

	High Democracy and Poor (N=950)			Low Democracy and Poor (N=1,766)		
Δ GDP p.c.	1.87	1.57	3.46	1.15	2.41	4.73
Harsh Drought Prevalence (W) ($PDSI < -4$)	0.0026	0.0208	0.1785	0.0051	0.0148	0.1809
Max T above 35 °C (W) ($TX35$)	0.0013	0.0049	0.0232	0.0008	0.0021	0.0292
Mean T in [9; 12) °C (TS_{9_12})	-0.00002	0.0009	0.0054	-0.00003	0.0004	0.0096
	1979-1999 (N=2,762)			2000-2019 (N=3,891)		
Δ GDP p.c.	1.16	2.71	4.63	2.13	1.94	3.68
Harsh Drought Prevalence (W) ($PDSI < -4$)	0.0034	0.0388	0.1596	0.0061	0.0162	0.1827
Max T above 35 °C (W) ($TX35$)	0.0002	0.0027	0.0224	0.0009	0.0020	0.0190
Mean T in [9; 12) °C (TS_{9_12})	-0.00004	0.0029	0.0138	0.0001	0.0007	0.0171

Note: Summary statistics of first difference of weather variables and GDP growth in percentage. Coefficients of weather variables are reported in Figure 5 and groups are described in the Notes to the Figure.

B.4. Additional Result Tables

Table B.6: Optimal LASSO selection of variables affecting GDP per capita growth under different fit criteria (baseline FE specification)

	BIC	AIC	OOS-Countries-R^2	OOS-Observations-R^2
Selected variables				
	Lag-1 GDP p.c. growth, Lag-2 GDP p.c. growth, Harsh Drought Prevalence$^{[W]}$, Max T °C above 35$^{[W]}$, Mean T °C in [9,12)	Lag-1 GDP p.c. growth, Lag-2 GDP p.c. growth, Harsh Drought Prevalence$^{[W]}$, Max T °C above 35$^{[W]}$, Mean T °C in [9,12), Longest Night Heat Wave$^{[W]}$, Lag-1 Mean T °C in [0,3)$^{[W]}$, Lag-1 Cold Spell Duration, Lag-2 Mean T °C in [3,6)$^{[W]}$, Lag-2 Cold Wave Days, Longest Night Cold Wave$^{[W]}$, 1-Day PPT Maximum, Drought Intensity, Lag-1 PPT Minimum$^{[W]}$, Lag-1 10 to 20 mm PPT, Lag-1 Day T °C Maximum, Lag-2 Balanced PPT Indicator, Lag-2 Mean T °C in [3,6), Cont'd Heavy PPT$^{[W]}$, Heavy PPT Maximum$^{[W]}$, Longest Dry Spell (.80)$^{[W]}$, Lag-1 Mean T °C in [24,27)$^{[W]}$, PPT Minimum$^{[W]}$, PPT Maximum$^{[W]}$, Cont'd Extreme PPT, Lag-1 Cont'd Wet Days$^{[W]}$, Lag-1 Harsh Drought Prevalence$^{[W]}$, Lag-1 Longest Dry Spell (.65)$^{[W]}$, Lag-2 Day Heatwave T °C$^{[W]}$, Lag-2 Longest Dry Spell (.80)$^{[W]}$, Lag-2 Very Wet Conditions Prevalence$^{[W]}$, Lag-2 Mean T °C in [0,3)$^{[W]}$, Lag-2 Mean T °C in [3,6)$^{[W]}$, Lag-2 Longest Dry Spell (.95), Lag-2 Longest Dry Spell (.5), Lag-2 Mean T °C in [21,24)	Lag-1 GDP p.c. growth, Lag-2 GDP p.c. growth, Harsh Drought Prevalence$^{[W]}$, Max T °C above 35$^{[W]}$, Mean T °C in [9,12), Longest Night Heat Wave$^{[W]}$, Lag-1 Mean T °C in [0,3)$^{[W]}$, Lag-1 Cold Spell Duration, Lag-2 Mean T °C in [3,6)$^{[W]}$, Lag-2 Cold Wave Days, Longest Night Cold Wave$^{[W]}$, 1-Day PPT Maximum, Drought Intensity, Lag-1 PPT Minimum$^{[W]}$, Lag-1 10 to 20 mm PPT, Lag-1 Day T °C Maximum, Lag-2 Balanced PPT Indicator, Lag-2 Mean T °C in [3,6)	Lag-1 GDP p.c. growth, Lag-2 GDP p.c. growth, Harsh Drought Prevalence$^{[W]}$, Max T °C above 35$^{[W]}$, Mean T °C in [9,12), Longest Night Heat Wave$^{[W]}$, Lag-1 Mean T °C in [0,3)$^{[W]}$, Lag-1 Cold Spell Duration, Lag-2 Mean T °C in [3,6)$^{[W]}$, Lag-2 Cold Wave Days, Longest Night Cold Wave$^{[W]}$, 1-Day PPT Maximum, Drought Intensity, Lag-1 PPT Minimum$^{[W]}$, Lag-1 10 to 20 mm PPT, Lag-1 Day T °C Maximum, Lag-2 Balanced PPT Indicator, Lag-2 Mean T °C in [3,6)
Number of Selected Variables	5	36	18	18
Optimal Penalty Weight (λ)	.0328	.0139	.019	.019

Notes: This table shows some results of the implementation of the LASSO to select the climate variables that are best to explain GDP per capita variations after accounting for country and year fixed effects. Each column corresponds to a different fit criteria and refers to the outcomes of implementing the LASSO after setting λ to optimize that specific fit criteria. For each column, the second row shows the list of the climate variables selected by the LASSO. The optimal value of λ is presented in the last row.

Table B.7: Optimal EN selection of variables affecting GDP per capita growth under different fit criteria (baseline FE specification)

	BIC	**AIC**	**OOS-Countries-R^2**	**OOS-Observations-R^2**
Selected variables				
	Lag-1 GDP p.c. growth, Lag-2 GDP p.c. growth, Harsh Drought Prevalence$^{[W]}$, Max T °C above 35$^{[W]}$, Mean T °C in [9,12)	Lag-1 GDP p.c. growth, Lag-2 GDP p.c. growth, Harsh Drought Prevalence$^{[W]}$, Max T °C above 35$^{[W]}$, Mean T °C in [9,12), Longest Night Heat Wave$^{[W]}$, Drought Intensity, Lag-1 Mean T °C in [0,3)$^{[W]}$, Lag-1 Cold Spell Duration, Lag-2 Mean T °C in [3,6)$^{[W]}$, Lag-2 Cold Wave Days	Lag-1 GDP p.c. growth, Lag-2 GDP p.c. growth, Harsh Drought Prevalence$^{[W]}$, Max T °C above 35$^{[W]}$, Mean T °C in [9,12), Longest Night Heat Wave$^{[W]}$, Longest Night Cold Wave$^{[W]}$, Drought Intensity, Cont'd Heavy PPT$^{[W]}$, 1-day PPT Maximum, Lag-1 Mean T °C in [0,3)$^{[W]}$, Lag-1 Cold Spell Duration, Lag-1 PPT Minimum$^{[W]}$, Lag-1 10 to 20 mm PPT, Lag-1 Day T °C Maximum, Lag-2 Mean T °C in [3,6)$^{[W]}$, Lag-2 Cold Wave Days, Lag-2 Balanced PPT Indicator, Lag-2 Mean T °C in [3,6), Lag-2 Mean T °C in [21,24)	Lag-1 GDP p.c. growth, Lag-2 GDP p.c. growth, Harsh Drought Prevalence$^{[W]}$, Max T °C above 35$^{[W]}$, Mean T °C in [9,12), Drought Intensity, Cont'd Heavy PPT$^{[W]}$, Longest Night Heat Wave$^{[W]}$, Longest Night Cold Wave$^{[W]}$, Heavy PPT Maximum$^{[W]}$, Longest Dry Spell$^{[W]}$, Mean T °C in [24,27)$^{[W]}$, Mean T °C above 30$^{[W]}$, PPT Maximum$^{[W]}$, PPT Minimum$^{[W]}$, 1-day PPT Maximum, Very Wet Day PPT, Cont'd Extreme PPT, Mean T °C in [6,9), Mean T °C in [18,21), Lag-1 Mean T °C in [0,3)$^{[W]}$, Lag-1 Cold Spell Duration, Lag-1 Wet Day PPT Variance, Lag-1 Cont'd Wet Days$^{[W]}$, Lag-1 Harsh Drought Prevalence$^{[W]}$, Lag-1 PPT Minimum$^{[W]}$, Lag-1 10 to 20 mm PPT, Lag-1 Longest Dry Spell (.65), Lag-1 Mean T °C in [0,3), Lag-1 Mean T °C in [9,12), Lag-1 Day T °C Maximum, Lag-2 Mean T °C in [3,6)$^{[W]}$, Lag-2 Cold Wave Days, Lag-2 Day Heat Wave T °C$^{[W]}$, Lag-2 # of Night Cold Waves$^{[W]}$, Lag-2 Longest Dry Spell (.80)$^{[W]}$, Lag-2 High Wetness Intensity$^{[W]}$, Lag-2 Very Wet Conditions Prevalence$^{[W]}$, Lag-2 Mean T °C in [0,3)$^{[W]}$, Lag-2 Mean T °C in [21,24)$^{[W]}$, Lag-2 Balanced PPT Indicator, Lag-2 Longest Dry Spell (.95), Lag-2 Longest Dry Spell (.80), Lag-2 Longest Dry Spell (.50), Lag-2 Mean T °C in [3,6), Lag-2 Mean T °C in [21,24)
Number of Selected Variables	5	11	21	46
Optimal Penalty Weight (λ)	.04	.03	.027	.062
Optimal LASSO Ratio (ϕ)	.8	.7	.648	.215

Notes: This table shows some results of the implementation of the Elastic-Net (EN) to select the climate variables that are best to explain GDP per capita variations after accounting for country and year fixed effects. Each column corresponds to a different fit criteria and refers to the outcomes of implementing the EN after setting λ and ϕ in equation (5) to optimize that specific fit criteria. For each column, the second row shows the list of the climate variables selected by the EN. The optimal values of λ and ϕ are presented in the last two rows, consecutively.

Table B.8: Optimal LASSO selection of variables under different model specifications and BIC

	Without Year Effects	**With Quadratic Trends**	**Balanced Sample with FE**
BIC			
	World GDP Growth, Lag-1 GDP p.c. growth, Lag-2 GDP p.c. growth, Harsh Drought Prevalence$^{[W]}$, Max T °C above 35$^{[W]}$	Lag-1 GDP p.c. growth, Harsh Drought Prevalence$^{[W]}$, Max T °C above 35$^{[W]}$	Lag-1 GDP p.c. growth, Lag-2 GDP p.c. growth, Harsh Drought Prevalence$^{[W]}$, Max T °C above 35$^{[W]}$, PPT Minimum$^{[W]}$
Number of Selected Variables	5	3	5
Optimal Penalty Weight (λ)	.039	.0285	.0372

Notes: This table shows some results of the implementation of the LASSO to select the climate variables that are best to explain GDP per capita variations after accounting for different fixed effects different specification. Each column corresponds to a different fixed-effect specification and refers to the outcomes of implementing the LASSO after setting λ to optimize the BIC. For each column, the second row shows the list of the climate variables selected by the LASSO. The optimal value of λ is presented in the last row.

Table B.9: Optimal LASSO selection affecting fiscal variables under BIC fit criteria

	Revenue	**Expenditure**	**Debt**
BIC			
	Lag-1 Revenue, Lag-2 Revenue, Harsh Drought Prevalence$^{[W]}$, Mean T °C in [24,27)$^{[W]}$, Cont'd Dry Days, Heavy PPT Maximum, PPT Minimum, Lag-1 Extremely Wet Day PPT$^{[W]}$, Lag-1 Longest Day Cold Wave$^{[W]}$, Lag-1 Harsh Drought Prevelance$^{[W]}$, Lag-1 Extremely Wet Day PPT, Lag-1 Cold Wave Days, Lag 1 Longest Dry Spell (.80), Lag-1 Mean T °C in [24,27)	Lag-1 GDP p.c. growth, Lag-1 Expenditure, Lag-2 Expenditure, Mean T °C in [-3,0)$^{[W]}$, Mean Wet Day PPT, Lag-1 Harsh Drought Prevelance$^{[W]}$	Lag-1 GDP p.c. growth, Lag-1 Debt, Lag-1 PPT Minimum
Number of Selected Variables	14	6	3
Optimal Penalty Weight (λ)	.0318	.0419	.0339

Notes: This table shows some results of the implementation of the LASSO to select the climate variables that are best to explain different fiscal variables after accounting for country and year fixed effects. Each column corresponds to a different fiscal variable and refers to the outcomes of implementing the LASSO after setting λ to optimize the BIC. For each column, the second row shows the list of the climate variables selected by the LASSO. The optimal value of λ is presented in the last row.

Table B.10: Climate variables selected by the LASSO using the AIC and their GDP effect under the baseline specification

	Variable	Est.		Variable	Est.		Variable	Est.
1	Lag-1 GDP per Capita Growth	0.220 (0.0325)	13	Max T °C above 35 (W)	-0.133 (0.0673)	25	Longest Night Cold Wave (W)	-0.0870 (0.0530)
2	Lag-2 GDP per Capita Growth	0.0898 (0.0197)	14	1-Day PPT Maximum	-0.127 (0.0560)	26	Lag-2 Longest Dry Spell (.5)	-0.0814 (0.0499)
3	PPT Maximum (W)	0.229 (0.0828)	15	Lag-2 Longest Dry Spell (.95)	0.120 (0.0741)	27	Heavy PPT Maximum (W)	0.0783 (0.0524)
4	Lag-1 Mean T °C in [0; 3) (W)	-0.219 (0.0601)	16	Lag-2 Mean T °C in [21; 24)	0.115 (0.0508)	28	Lag-2 Cold Wave Days	-0.0773 (0.0531)
5	Lag-2 Longest Dry Spell (.80) (W)	-0.219 (0.0869)	17	Longest Night Heat Wave (W)	-0.108 (0.0350)	29	Lag-2 Very Wet Conditions (W)	-0.0765 (0.0436)
6	Lag-2 Longest Dry Spell (.80)	0.187 (0.0851)	18	Lag-1 Longest Dry Spell (.65)	0.108 (0.0639)	30	Lag-2 Mean T °C in [3; 6)	-0.0713 (0.0810)
7	Cont'd Heavy PPT (W)	-0.165 (0.0701)	19	Lag-1 Day T °C Maximum	0.103 (0.0439)	31	Drought Intensity	-0.0646 (0.0601)
8	Mean T °C in [9; 12)	0.165 (0.0418)	20	PPT Minimum (W)	-0.101 (0.0769)	32	Lag-1 Harsh Drought Prevalence (W)	0.0549 (0.0530)
9	Harsh Drought Prevalence (W)	-0.164 (0.0613)	21	Longest Dry Spell (.80) (W)	0.0977 (0.0673)	33	Lag-2 Balanced PPT Indicator	0.0546 (0.0541)
10	Lag-2 Mean T °C in [0; 3) (W)	-0.163 (0.0608)	22	Lag-2 Day Heat Wave T °C (W)	0.0917 (0.0583)	34	Cont'd Extreme PPT	-0.0472 (0.0630)
11	Lag-1 Cold Spell Duration	0.160 (0.0658)	23	Mean T °C in [24; 27) (W)	0.0900 (0.0528)	35	Lag-1 PPT Minimum (W)	0.0455 (0.0687)
12	Lag-1 10 to 20 mm PPT	0.138 (0.0607)	24	Lag-1 Cont'd Wet Days (W)	-0.0872 (0.0510)	36	Lag-2 Mean T °C in [3; 6) (W)	-0.0455 (0.0734)
	Observations	6,653		R-squared	0.281		Within R-squared	0.114

Notes: The table lists the variables selected by the LASSO after a random search for lambda to maximize the AIC. The Est. column indicates the coefficient estimates from a linear regression with country and year fixed effects. All climate variables are first-differenced and standardized. (W) indicates population-weighted variables. Standard errors are clustered by country and reported in brackets.

Table B.11: Climate variables selected by the LASSO using the out-of-sample within R-squared and their GDP effect under the baseline specification

	Variable	Est.		Variable	Est.		Variable	Est.
1	Lag-1 GDP per Capita Growth	0.217	7	Lag-1 Mean T °C in [0; 3) (W)	-0.131	13	Lag-1 PPT Minimum (W)	0.0885
		(0.0333)			(0.0381)			(0.0683)
2	Lag-2 GDP per Capita Growth	0.0897	8	Lag-1 Day T °C Maximum	0.106	14	Lag-2 Cold Wave Days	-0.0795
		(0.0199)			(0.0412)			(0.0542)
3	Harsh Drought Prevalence (W)	-0.169	9	Longest Night Heat Wave (W)	-0.105	15	Lag-2 Balanced PPT Indicator	0.0788
		(0.0600)			(0.0342)			(0.0505)
4	Max T °C above 35 (W)	-0.162	10	1-Day PPT Maximum	-0.104	16	Drought Intensity	-0.0665
		(0.0709)			(0.0477)			(0.0568)
5	Lag-1 Cold Spell Duration	0.158	11	Lag-2 Mean T °C in [3; 6) (W)	-0.104	17	Lag-1 10 to 20 mm PPT	0.0616
		(0.0676)			(0.0777)			(0.0580)
6	Mean T °C in [9; 12)	0.151	12	Longest Night Cold Wave (W)	-0.0962	18	Lag-2 Mean T °C in [3; 6)	-0.0450
		(0.0412)			(0.0533)			(0.0818)
	Observations	6,653		R-squared	0.273		Within R-squared	0.105

Notes: The table lists the variables selected by the LASSO after a random search for lambda to maximize the out-of-sample within R-squared. In this case, we obtain the same variable selection whether we randomly assign countries (and all their observations) to the test set or if we randomly assign observations to the test without accounting for the country panel structure. The Est. column indicates the coefficient estimates from a linear regression with country and year fixed effects. All climate variables are first-differenced and standardized. (W) indicates population-weighted variables. Standard errors are clustered by country and reported in brackets.

B.5. Additional Figures

Figure B.2: Selection of climate variables impacting GDP (specification without year effects)

(a) using the AIC (b) using the BIC (c) using the OOS within R2

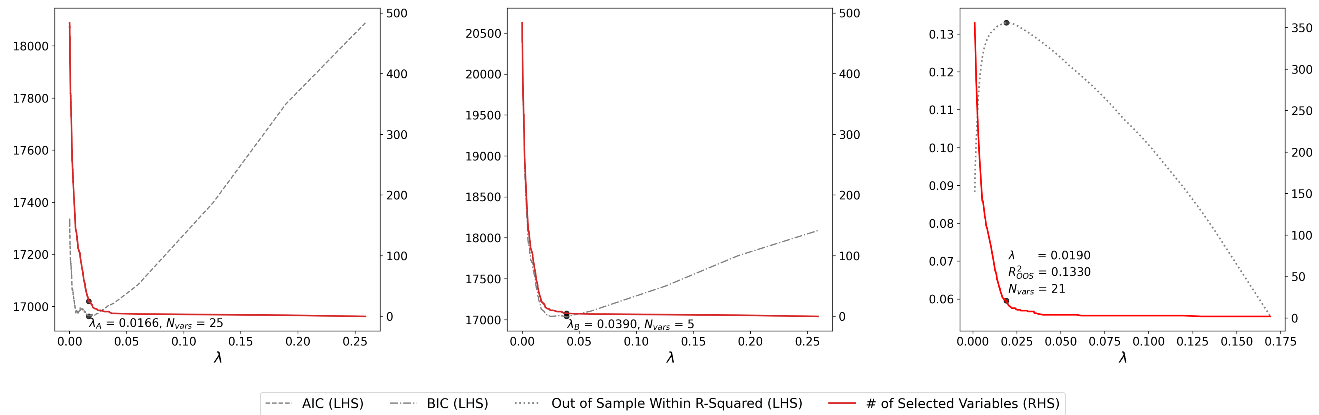

Note: GDP per capita growth is the dependent variable and the specification has country effects and world growth. See the notes of the following graph for more details.

Figure B.3: Selection of climate variables impacting GDP (specification with quadratic trends)

(a) using the AIC (b) using the BIC (c) using the OOS within R2

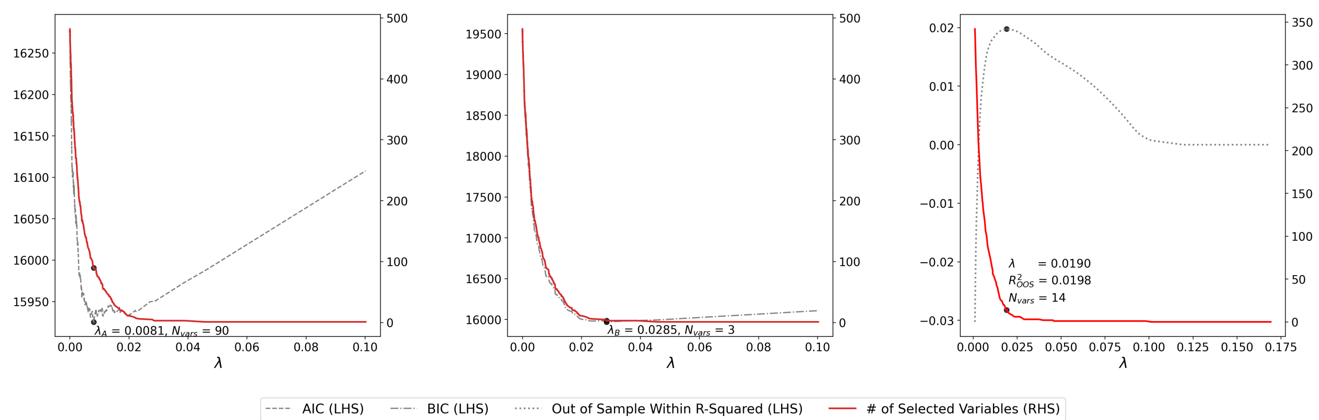

Note: The figures show the results of implementing the LASSO for different penalty parameters λ. The red lines are similar in every panel and show how the number of selected variables vary with λ. The grey dashed lines in each panel show the variation of different criteria with λ. The out-of-sample (OOS) within R-squared is calculated on a sub-sample of countries (evaluation set) based on coefficients estimated on the rest of countries (training set) as explained in the main text. The dots indicate the different selection outcomes given by the local optimum for each criteria respectively. The estimated model has GDP per capita growth as the dependent variable and includes country quadratic trends and year effects.

Figure B.4: Selection of climate variables impacting GDP (balanced sample with FE)

(a) using the AIC (b) using the BIC (c) using the OOS within R2

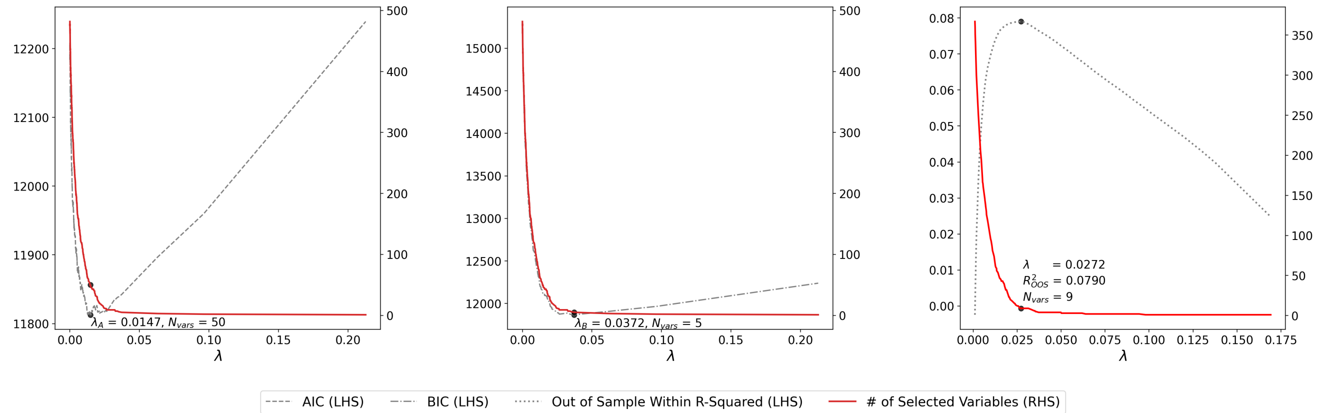

Note: GDP per capita growth is the dependent variable and the specification with country and year effects was estimated on the balanced sample for 1984-2019. See the notes of the following graph for more details.

Figure B.5: Selection of climate variables impacting government revenue

(a) Selection using the AIC (b) Selection using the BIC

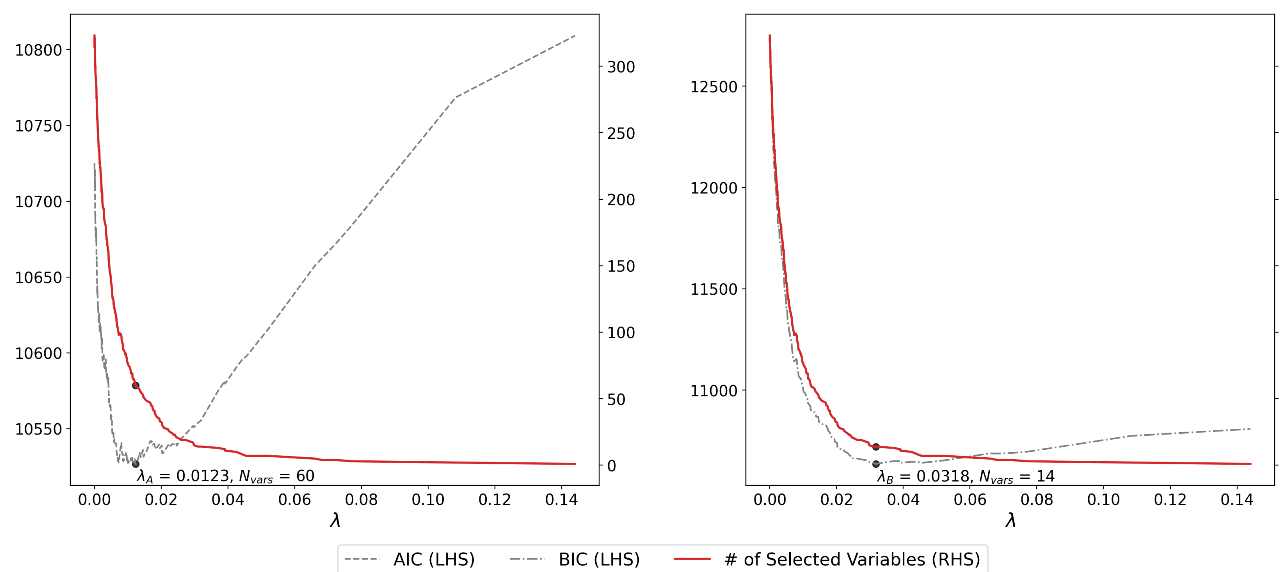

Note: The figures show the results of implementing the LASSO for different penalty parameters λ. The red lines are similar in every panel and show how the number of selected variables vary with λ. The grey dashed lines in each panel show the variation of different criteria with λ. The within R-squared is calculated on a sub-sample of countries (evaluation set) based on coefficients estimated on the rest of countries (training set) as explained in the main text. The dots indicate the different selection outcomes given by the local optimum for each criteria respectively. The estimated model has the ratio of government revenue to GDP as the dependent variable and includes country and year effects.

Figure B.6: Selection of climate variables impacting government expenditure

(a) Selection using the AIC (b) Selection using the BIC

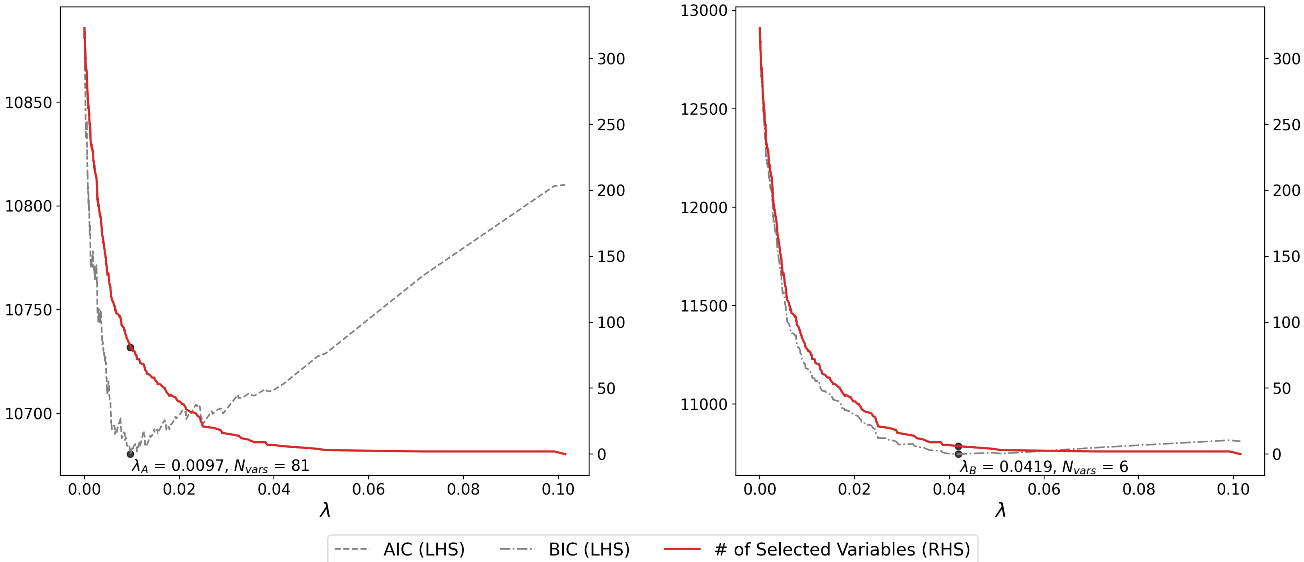

Note: The estimated model has the ratio of government expenditure to GDP as the dependent variable and includes country and year effects. See the notes of the following graph for more details.

Figure B.7: Selection of climate variables impacting government debt

(a) Selection using the AIC (b) Selection using the BIC

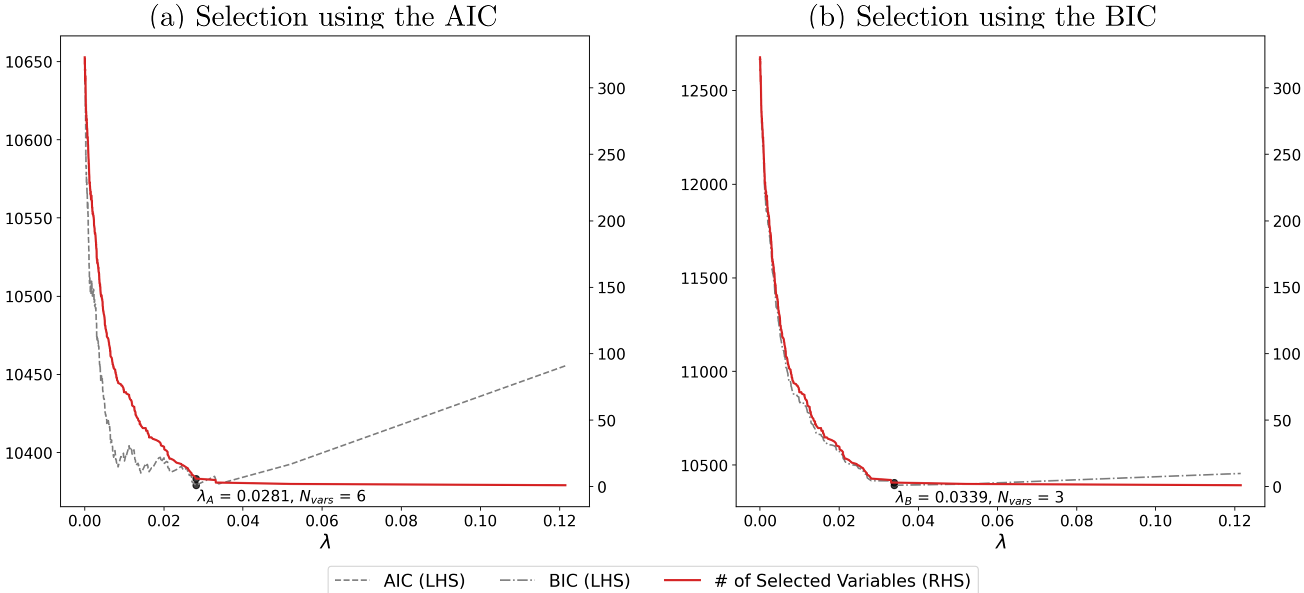

Note: The figures show the results of implementing the LASSO for different penalty parameters λ. The red lines are similar in every panel and show how the number of selected variables vary with λ. The grey dashed lines in each panel show the variation of different criteria with λ. The within R-squared is calculated on a sub-sample of countries (evaluation set) based on coefficients estimated on the rest of countries (training set) as explained in the main text. The dots indicate the different selection outcomes given by the local optimum for each criteria respectively. Government debt to GDP is the dependent variable and the specification has country and year effects.

B.6. LASSO and Elastic-Net Implementation

In this appendix, we detail our implementation of the various algorithms covered in the paper, with an emphasis on the technical steps and the specific software and functions that we use.

We define X as the matrix containing (first differenced) right hand side variables, excluding fixed effects, but including relevant lags of the dependent variable Δy. For details on the lags used in each regression model, please refer to the main article. We designate F as the matrix of fixed effects, which varies according to the model specification. Specifically, F can encompass:

a) Country and year fixed effects, or

b) Only country fixed effects, or

c) Country fixed effects, year fixed effects, and country quadratic dummies.

The organization of these matrices is such that rows represent individual observations and columns correspond to variables. To ensure compatibility with our Python-based feature selection algorithm (Python version 3.9 or higher), we remove any missing observations.

Using this notation, the regression model incorporating all variables can be summarized as shown in equation (B.1), which is the same as equation (2) in the main text but using different notations to single-out and combine fixed effects under one matrix F. Note that we have omitted subscripts from the fixed effects matrix F to indicate its flexibility; depending on the specification, F may contain only country-related information (i) and/or year-related information (t).

$$\Delta y_{it} = X_{it}\beta + F\theta + \varepsilon_{it} \tag{B.1}$$

Before constructing the fixed effects matrix F, we first eliminate outlier observations for the dependent variable. Specifically, any observation Δy_{it} that deviates by more than 5 standard deviations from the mean $\overline{\Delta y_{it}}$ is removed as described in section 3.3 in the main text. Because the LASSO penalizes the value of the coefficients, the scales of the parameters can affect the selection. Therefore, we standardize each column of X_{it} to have 0 mean and a standard deviation of 1. After this preprocessing step, we proceed to generate the F matrix.

The variable selection algorithm focuses on the variables within X_{it}. However, theoretical considerations mandate the inclusion of fixed effects in the regression model. To reconcile these aspects, we force the presence of fixed effects in the regression. We do so by first subtracting $F(F'F)^{-1}F'\Delta y$ from both sides of the equation.

$$\Delta y_{it} - F(F'F)^{-1}F'\Delta y = X_{it}\beta + F\theta - F(F'F)^{-1}F' \underbrace{(X_{it}\beta + F\theta + \varepsilon_{it})}_{\Delta y} + \varepsilon_{it}$$

$$\underbrace{(I - F(F'F)^{-1}F')\Delta y_{it}}_{\Delta\tilde{y}_{it}} = \underbrace{(I - F(F'F)^{-1}F')X_{it}}_{\tilde{X}_{it}}\beta + \underbrace{F\theta - F\underbrace{(F'F)^{-1}F'F}_{I}\theta}_{0} + \underbrace{(I - F(F'F)^{-1}F')\varepsilon_{it}}_{u_{it}}$$

$$\implies \Delta\tilde{y}_{it} = \tilde{X}_{it}\beta + u_{it} \tag{B.2}$$

The Frisch-Waugh-Lowell theorem implies that the estimations based on equations (B.1) and (B.2) result in the same estimate for β. Consequently, performing the selection algorithm after the above transformation effectively incorporates the fixed effects into the regression model.

As elaborated in the main text, our objective is to select a subset of columns from the matrix $\tilde{X}_{it}$. To achieve this, we employ LASSO and Elastic-Net methods, which are detailed in the subsequent sections. The analyses are conducted using version 1.2.2 of the Scikit-Learn package in Python. To ensure replicability due to the random sampling described later, we set the random seed using the numpy package, version 1.25.0. All computations are performed on a Windows 11 machine with a 13th Gen Intel(R) Core(TM) i7-13700 processor, operating at 2.10 GHz.

B.6.1 LASSO

As explained in Section 2.3 in the main text, the LASSO aims to solve equation (4), that is to minimize the following equation:

$$\min_{\beta} \quad \Delta\tilde{y}_{it} - \tilde{X}_{it}\beta + \lambda \sum_{j=1}^{K} |\beta_j| \tag{B.3}$$

where the hyperparameter λ weighs the penalty term, which is the sum of the absolute values of the coefficients β_j. K denotes the number of columns in the matrix $\tilde{X}_{it}$.

The penalty term encourages some coefficients to shrink towards zero. As λ increases, the penalty term gains more weight, leading to more coefficients becoming zero. Conversely, a smaller λ results in fewer coefficients shrinking to zero. Coefficients that remain non-zero are those for which the reduction in standard error outweighs the penalty incurred by their inclusion in the regression.

To determine the optimal value of the hyperparameter λ, we explore four approaches:

1. Minimizing the Bayesian Information Criterion (BIC),
2. Minimizing the Akaike Information Criterion (AIC),

3. Maximizing the average out-of-sample R^2 using 5-fold cross-validation (and since we remove fixed-effects, this R^2-metric corresponds to what is commonly defined as the *within* R^2). In this method, observations are randomly divided into five bins without considering the panel structure of the data,

4. Maximizing the average out-of-sample R^2 with a modified 5-fold cross-validation approach that respects the panel structure (and again, since we remove fixed-effects, this R^2-metric corresponds to what is commonly defined as the *within* R^2). Specifically, countries are divided into five bins, and observations for these countries are used in each fold separately.

For the first two approaches, we employ the built-in `LassoLarsIC()` function available in Scikit-Learn. This function utilizes the Least Angle Regression (LARS) algorithm for LASSO variable selection, as opposed to Scikit-Learn's main LASSO implementation, which relies on a gradient-descent algorithm. Both methods aim to solve the same optimization problem but take different computational routes.

For the third approach, we employ 5-fold cross-validation. In k-fold cross-validation, the dataset is randomly divided into k subsets of equal (or nearly equal) size called folds. One fold is reserved as the test set, and the model is trained on the remaining $k-1$ folds. This process is repeated k times, each time with a different fold serving as the test set. The performance metric, in our case the out-of-sample R^2, is then averaged across all k iterations.

We employ Scikit-Learn's `RandomizedSearchCV()` function to conduct the 5-fold cross-validation. We perform the cross-validation for 200 distinct penalty weights, leading to a total of 1,000 model fits. These penalty weights are drawn from a half-normal distribution with a location parameter (loc) of 0.001 and a scale parameter of 0.05.

For the fourth approach, we use NumPy's `random.choice()` function to divide the countries into 5 folds: four folds contain 41 countries each, while the fifth contains 39 countries. We then proceed in a manner similar to the k-fold cross-validation described above. Specifically, for each of 200 distinct penalty weights, we fit the model using observations from four folds, reserving one fold as the test set to calculate the out-of-sample R^2. Each penalty weight is evaluated five times—once for each fold serving as the test set—and the average R^2 is computed. The penalty weight yielding the highest average R^2 is then selected.

B.6.2 Elastic-Net

Using the notations of this section, the Elastic-Net optimization problem covered in equation (5) in the main text can be expressed as follows (note that ϕ would correspond to α in the Scikit-Learn package's notations):

$$\min_{\beta} \quad \frac{1}{2N}(\Delta\tilde{y}_{it} - \tilde{X}_{it}\beta) + \lambda\phi\sum_{j=1}^{K}|\beta_j| + \lambda\frac{1-\phi}{2}\sum_{j=1}^{K}\beta_j^2 \tag{B.4}$$

In equation (B.4), we have two hyperparameters, λ and ϕ. The range of ϕ is between 0 and 1, and it determines the balance between the penalty terms associated with the LASSO and the Ridge. Increasing ϕ promotes sparsity in the solution. Likewise, increasing λ enhances sparsity, given that $\phi \neq 0$. However, the selection of variables may differ depending on the approach taken. To determine the optimal ϕ and λ combination, we employ the same approach as we did for the LASSO and separately consider 4 different fit criteria.

Unlike in the LASSO case, there is no built-in function available to minimize the BIC and AIC in the case of the Elastic-Net. As a result, we modify the source codes of the `LassoLarsIC()` to make it compatible with the Elastic-Net.[35] Since the faster LARS algorithm is not available for the Elastic-Net, we resort to the gradient descent algorithm. Consequently, we do not explore every possible combination of ϕ and λ. We consider 9 distinct values for ϕ (ranging from 0.1 to 0.9 with increments of 0.1) and 16 values for λ (0.0025, 0.005, 0.01, 0.02, 0.03, 0.04, 0.05, 0.06, 0.07, 0.08, 0.09, 0.1, 0.15, 0.2, 0.25, 0.3). This results in a total of $9 \times 16 = 144$ unique combinations. For each of these 144 combinations, we calculate the AIC and BIC values using the formulas:

$$AIC = N \times log(2\pi\hat{\sigma}_u^2) + \frac{RSS}{\hat{\sigma}_u^2} + 2 \times \text{DoF} \tag{B.5}$$

$$BIC = N \times log(2\pi\hat{\sigma}_u^2) + \frac{RSS}{\hat{\sigma}_u^2} + log(N) \times \text{DoF} \tag{B.6}$$

We use the residual sum of squares (RSS) obtained after making predictions with the Elastic-Net, and the degrees of freedom (DoF) are equal to the number of non-zero coefficients after the Elastic-Net. N is the number of observations, and $\hat{\sigma}_u^2$ is the estimated variance of the error term in equation (B.2). The error term is estimated before the selection using all variables in the X_{it} matrix as in the source codes of `LassoLarsIC()` function.

For maximizing the out-of-sample within R^2 using k-fold cross-validation in the case when the observations are randomly allocated without considering the panel structure, we again utilize Scikit-Learn's `RandomizedSearchCV()` function. We sample the ϕ parameter from a uniform distribution ranging from 0.1 to 0.9, and the λ parameter from a half-normal distribution with a location parameter (loc) of 0.001 and a scale parameter of 0.5. We consider 200 distinct combinations, resulting in a total of 1,000 model fits across 5 folds.

Lastly, maximizing the out-of-sample within R^2 using k-fold cross-validation in the case when observations are randomly allocated factoring in the country panel structure, we employ NumPy's `random.choice()` function to partition the countries into 5 folds. Four of these folds contain 41 countries each, and the fifth contains 39 countries. To prevent corner solutions, we use a smaller scale parameter for the half-normal distribution this time. Specifically, ϕ is sampled from a uniform distribution ranging between 0.1 and

[35]The source codes can be found in `https://github.com/scikit-learn/scikit-learn/blob/main/sklearn/linear_model/_least_angle.py#L2280`, after lines 2089 as of November 2023.

0.9, while λ is drawn from a half-normal distribution with a location parameter (loc) of 0.001 and a scale parameter of 0.1 (as opposed to 0.5 used in previous exercises).

For the two implementation based on the out-of-sample within R^2, we implement the EN five times for each combination of penalty weights, once with each fold serving as the test set. For each combination, we compute the average R^2. The combination of penalty weights that maximizes this average R^2 is then determined to be the optimal combination.

References

Abatzoglou, J. T., S. Z. Dobrowski, S. A. Parks, and K. C. Hegewisch (2018). Terraclimate, a high-resolution global dataset of monthly climate and climatic water balance from 1958–2015. Scientific data 5(1), 1–12.

Dai, A., K. E. Trenberth, and T. Qian (2004). A Global Dataset of Palmer Drought Severity Index for 1870-2002: Relationship with Soil Moiusture and Effects of Surface Warming. Journal of Hydrometeorology 5, 1117–1130.

IPCC (2021a). Atlas. In Climate Change 2021: The Physical Science Basis. Contribution of Working Group I to the Sixth Assessment Report of the Intergovernmental Panel on Climate Change.

IPCC (2021b). Summary for policymakers. In Climate Change 2021: The Physical Science Basis. Contribution of Working Group I to the Sixth Assessment Report of the Intergovernmental Panel on Climate Change. Cambridge University Press.

Kim, Y.-H., S.-K. Min, X. Zhang, J. Sillmann, and M. Sandstad (2020). Evaluation of the CMIP6 multi-model ensemble for climate extreme indices. Weather and Climate Extremes 29.

Lai, Peiyu abd Zhang, M., Z. Ge, B. Hao, Z. Song, J. Huang, M. Ma, H. Yang, and X. Han (2020). Responses of Seasonal Indicators to Extreme Droughts in Southwest China. Remote Sensing 12.

Mérel, P. and M. Gammans (2021). Climate econometrics: Can the panel approach account for long-run adaptation? American Journal of Agricultural Economics 103(4), 1207–1238.

Palmer, W. C. (1965). Meteorological Drought. Research Paper, U.S. Weather Bureau.

Perkins, S. E. and L. V. Alexander (2013). On the Measurement of Heatwaves. Journal of Climate 26.

Schlenker, W. and M. J. Roberts (2009). Nonlinear temperature effects indicate severe damages to US crop yields under climate change. Proceedings of the National Academy of sciences 106(37), 15594–15598.